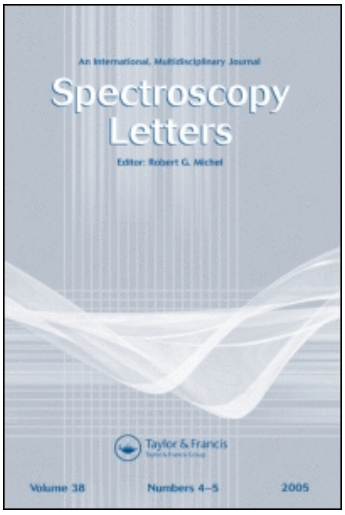


**Spectroscopy Letters**
Publication details, including instructions for authors and subscription information:
http://www.informaworld.com/smpp/title~content=t713597299

# The Application of Two-dimensional Fluorescence Correlation Spectroscopy on the Interaction Between Bovine Serum Albumin and Paeonolum in the Presence of Fe(III)

Changyun Chen[a]; Bingren Xiang[b]; Liyan Yu[b]; Teng Wang[b]; Bo Zhao[c]
[a] Department of Chemistry, Nanjing Xiaozhuang University, Nanjing, Jiangsu Province, People's Republic of China [b] Center for Instrumental Analysis (Key Laboratory of Drug Quality Control and Pharmacovigilance, Ministry of Education), China Pharmaceutical University, Nanjing, Jiangsu Province, People's Republic of China [c] Department of Chemistry, Nanjing Normal University, Nanjing, Jiangsu Province, People's Republic of China

**To cite this Article** Chen, Changyun , Xiang, Bingren , Yu, Liyan , Wang, Teng and Zhao, Bo(2008) 'The Application of Two-dimensional Fluorescence Correlation Spectroscopy on the Interaction Between Bovine Serum Albumin and Paeonolum in the Presence of Fe(III)', Spectroscopy Letters, 41: 8, 385 — 392
**To link to this Article: DOI:** 10.1080/00387010802428773
**URL:** http://dx.doi.org/10.1080/00387010802428773

*Spectroscopy Letters*, 41:385–392, 2008

ISSN: 0038-7010 print/1532-2289 online
DOI: 10.1080/00387010802428773

Taylor & Francis
Taylor & Francis Group

# The Application of Two-dimensional Fluorescence Correlation Spectroscopy on the Interaction Between Bovine Serum Albumin and Paeonolum in the Presence of Fe(III)

**Changyun Chen[1], Bingren Xiang[2], Liyan Yu[2], Teng Wang[2], and Bo Zhao[3]**

[1]Department of Chemistry, Nanjing Xiaozhuang University, Nanjing, Jiangsu Province, People's Republic of China
[2]Center for Instrumental Analysis (Key Laboratory of Drug Quality Control and Pharmacovigilance, Ministry of Education), China Pharmaceutical University, Nanjing, Jiangsu Province, People's Republic of China
[3]Department of Chemistry, Nanjing Normal University, Nanjing, Jiangsu Province, People's Republic of China



**ABSTRACT** The effect of $Fe^{3+}$ on the interaction between bovine serum albumin (BSA) and paeonolum (PAL), which was extracted from the traditional Chinese herb, *Paeonia suffruticosa Andr*, was investigated by UV and fluorescence spectroscopy. Two-dimensional correlation spectroscopy was applied to the analysis of fluorescence spectra. The results of spectroscopic measurements suggested that PAL had a strong ability to quench the intrinsic fluorescence of BSA through static quenching procedure in the presence of Fe(III). Thermodynamic parameter enthalpy changes ($\Delta H$) and entropy changes ($\Delta S$) were calculated. The binding parameters including binding constant ($K$), and the distance ($r$) between PAL and BSA were evaluated on the basis of the theory of Föster energy transfer. Owing to the spectral resolution enhancement in 2D correlation spectroscopy, the structure change of PAL–$Fe^{3+}$ can be observed.

**KEYWORDS** bovine serum albumin, Fe(III), fluorescence quenching, paeonolum, two-dimensional fluorescence correlation spectroscopy, UV absorption spectroscopy

## INTRODUCTION

The interactions between biomacromolecules and medicines have attracted great interest in recent years.[1–3] Among biomacromolecules, serum albumin is the major soluble protein constituent of the circulatory system and has many physiologic functions. The most outstanding function of albumins is that they can serve as depot protein and transport protein for many exogenous compounds and are capable of binding an extraordinarily diverse range of metabolites, medicines, and other organic compounds.[4,5] The interaction between protein and medicine may results in the formation of stable protein–medicine complex, which has important effect on the absorption, distribution, and

Received 13 December 2007; accepted 28 April 2008.

Address correspondence to Changyun Chen, Department of Chemistry, Nanjing Xiaozhuang University, Beiwei Road 41, Nanjing 210017, Jiangsu Province, People's Republic of China. E-mail: yhjiangccy@126.com

metabolism of medicine *in vivo*. Therefore, studies on the binding of medicine with protein will facilitate interpretation of the metabolism and transporting process of medicine and will help to explain the relationship between structure and function of protein. In this regard, bovine serum albumin (BSA) has been studied extensively, partly because of its structural homology with human serum albumin (HSA).

The primary structure of BSA has been well known for a long time, and its tertiary structure was determined by x-ray crystallography.[6,7] Therefore, a number of studies have been focused on the multifunctional binding properties of BSA, which binds a wide variety of molecules, but less attention has been paid to the active components of traditional Chinese herbs. The binding of metal ions, such as $Cu^{2+}$, $Zn^{2+}$, $Ni^{2+}$, and so forth, to serum albumin has also been widely reported, even the interaction between BSA and a few kinds of medicine, such as daunorubicin[8] and 5-fluorouracil[9] in the presence of metal ions. However, the influence of metal ions on the interaction between the active components of traditional Chinese herbs and BSA is less reported. Trace metal elements exist always in organisms and play important roles in the growth of organisms, cell division, and protein synthesis.[10] Their pharmacologic functions cannot be neglected. But the exact role metal ions play in the organism and the function of various metal ions coexisting in traditional Chinese herbs is still not completely clear. Thus it is necessary to study how the metal ions participate in the interaction between albumin serum and active components of traditional Chinese herbs.

Paeonolum (Fig. 1) is the major bioactive components of the traditional Chinese herb *Paeonia suffruticosa Andr*, which has many pharmaceutical properties such as sedation, hypnosis, antisepsis, anti-inflammatory, antioxidant, and so on. In our previous research, we have reported the interaction between BSA and paeonolum in the absence of metal ions at physiologic pH.[11] In this paper, the effect of $Fe^{3+}$ on the interaction between BSA and paeonolum were primarily studied by means of UV and fluorescence spectroscopy.

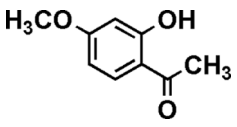


**FIGURE 1** **Molecular structure of paeonolum.**

Generalized two-dimensional (2D) correlation spectroscopy[12–15] was originally proposed by Noda in 1993 as an extension of his original 2D-correlation sprctroscopy. 2D correlation spectroscopy allows us to monitor spectral intensity fluctuation as a function of any physical variable (e.g., time, temperature, pressure, distance, or concentration). Thus, the temperature dependence of vibrational spectra can be studied. Owing to the enhancement of the spectral resolution by spreading the peaks over the second dimension, it is possible to identify the bands not readily seen in the original data set. Additionally, 2D correlation spectra provide information about the sequential order of the spectral intensity changes of different molecular segments in the course of the external perturbation. Two-dimensional correlation method also seems to be useful for analyzing complicated fluorescence spectra. Therefore, we tried to introduce the 2D correlation method to the field of fluorescence spectroscopy: it has the capability of resolution enhancement, enables one to correlate many bands to each other, and makes the band assignment more feasible. Using 2D spectroscopy, it is also possible to probe the specific order of chemical functional changes upon perturbation and to perform detailed dynamics study of molecule vibration.

## MATERIALS AND METHODS

### Materials and Reagents

Paeonolum (PAL) was obtained from the National Institute for Control of Pharmaceutical and Biological Products (Beijing, China). BSA and Tris were purchased from Sigma (St. Louis, MO). NaCl solution (0.1 mol/L) was used to keep the ionic strength, and 0.05 mol/L Tris-HCl buffer solution was selected to keep the pH of the solution at 7.4. The working solution PAL ($9.7 \times 10^{-7}$ mol/L) and BSA ($9.8 \times 10^{-7}$ mol/L) was prepared by dissolving in Tris-HCl buffer solution and kept in the dark at 4°C. All other reagents and solvents were of analytical reagent grade and used without further purification. All aqueous solutions were prepared using fresh double-distilled water.

### Apparatus

A LS-50B fluorescence spectrophotometer (Perkin Elmer, Boston, MA) equipped with 1.0-cm quartz cell was used to measure the fluorescence spectra and

the fluorescence intensity, and the absorption spectra were recorded on a TU-1901 spectra-photometer (Puxi, Beijing, China). The pH measurements were carried out on a pHS-25 acidometer (Leici, Shanghai, China), and the temperature was controlled by an HH-4 digital thermostatic waterbath (Ronghua, Jintan, China).

## Procedures

The PAL–$Fe^{3+}$ solution was prepared by mixing the solution of metal ions and PAL in the buffer solution, and appropriate quantities were transferred to a 10-mL flask. Then, 3.0 mL BSA solution was added and diluted to 10 mL with fresh double-distilled water. The resultant mixture was subsequently ultrasonicated for 5 min and incubated at 290.15, 300.15, and 310.15 K for 15 min. The emission spectra were recorded between 300 and 500 nm under the excitation at wavelength of 285 nm. The excitation and emission slit widths were set at 5.0 nm.

The UV spectra were obtained by scanning the solution on the spectrophotometer in the wavelength range 200–500 nm. The operations were carried out at room temperature.

# RESULTS AND DISCUSSION

## Fluorescence Quenching Spectra

The fluorescence spectra of BSA quenched by PAL at different PAL concentrations with metal ions are shown in Fig. 2. It was observed that the fluorescence intensity of BSA decreased regularly with the concentration increase of the PAL–$Fe^{3+}$ solution, but there was no significant $\lambda_{em}$ shift with the addition of the PAL–$Fe^{3+}$ solution. Apparently, PAL–$Fe^{3+}$ has a quench for the fluorescence of BSA, and there are interactions and energy transfer among PAL–$Fe^{3+}$ and BSA. These data indicated that PAL could interact with BSA and quench its intrinsic fluorescence in the presence of Fe(III).

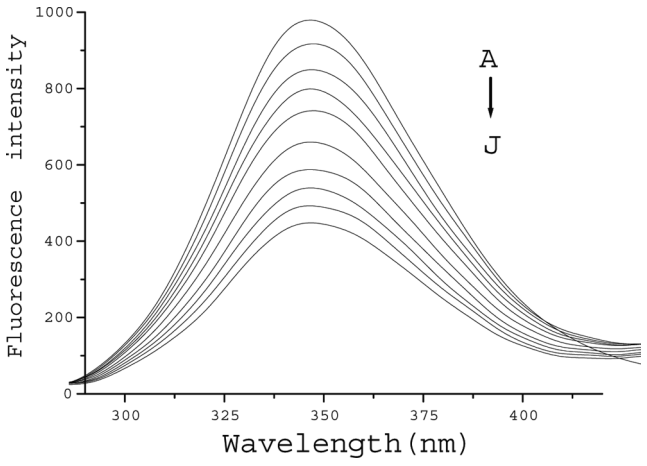


**FIGURE 2** Fluorescence of BSA quenched by PAL in the presence of $Fe^{3+}$ at 300.15 K. $C_{BSA} = 9.8 \times 10^{-7}$ mol/L, $C_{Fe(III)} = 9.7 \times 10^{-7}$ mol/L, $C_{PAL}$ from A to J 0, 14.55, 29.10, 43.65, 58.20, 87.30, 116.40, 145.50, 174.60, and 203.70 ($\times 10^{-7}$ mol/L).

## Quenching Mode of BSA Intrinsic Fluorescence

Fluorescent quenching can occur in two different mechanisms: static quenching and dynamic quenching. Static and dynamic quenching can be distinguished by their different dependence on temperature and excited-state lifetime. Higher temperatures will result in faster diffusion and hence larger amounts of collision quenching. Meanwhile, higher temperature will also result in the dissociation of weakly bound complexes and hence smaller amounts of static quenching. For dynamic quenching, the mechanism can be described by the Stern–Volmer equation[16]:

$$F_0/F = 1 + K_q\tau_0[Q] = 1 + K_{SV}[Q] \qquad (1)$$

where $F_0$ and $F$ represent the steady-state fluorescence intensities in the absence and presence of quencher, respectively, and $[Q]$ is the concentration of quencher. $K_q$ is the quenching rate constant of biomolecule, and $\tau_0$ is the average lifetime of biomolecule without the quencher, and its value is $10^{-8}$ s.[17] $K_{SV}$ is the Stern–Volmer quenching constant, which was determined by linear regression of Stern–Volmer equation.

To clarify the quenching mechanism, it was first assumed that the interactions proceed in a dynamic way. The temperature-dependent fluorescence quenching of BSA by PAL–$Fe^{3+}$ was then carried out. The Stern–Volmer plots at different temperatures are shown in Fig. 3. From the experimental data, the corresponding quenching constants for the interaction between PAL–$Fe^{3+}$ and BSA were calculated by the Stern–Volmer equation and are listed in Table 1. The higher quench constant obtained in the presence of Fe(III) might result from the interaction of metal ion with the drug, forming a complex, and then the complex interacted with the protein.

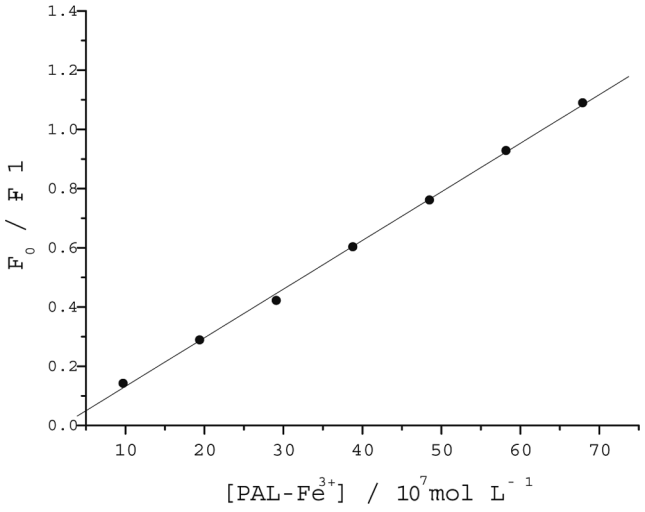


**FIGURE 3** **The Sterm–Volmer curves of fluorescence quenching of BSA by PAL–$Fe^{3+}$ at 300.15 K.**

According to the literature,[17] for dynamic quenching, the maximum scattering collision quenching constant of various quenchers with the biopolymer is $2.0 \times 10^{10}\,\mathrm{L\,mol^{-1}\ s^{-1}}$, and the $K_{SV}$ increases with increasing temperature. Considering that in our experiment the rate constant of the protein quenching procedure initiated by PAL–$Fe^{3+}$ is much greater than $2.0 \times 10^{10}\,\mathrm{L\,mol^{-1}\ s^{-1}}$ and that the $K_{SV}$ decreased with increasing temperature, it can be concluded that the quenching is not initiated by dynamic quenching, but probably by static quenching.

## Binding Constant and Binding Sites Number

For static quenching, the relationship between fluorescence quenching intensity and the concentration of quenchers can be described by the binding constant formula[18]:

$$\lg[(F_0 - F)/F] = \lg K_a + n\lg[Q] \qquad (2)$$

where $K_a$ is the binding constant, and $n$ is the number of binding sites. After the fluorescence quenching intensities on BSA at 347 nm were measured, the double-logarithm algorithm was assessed by Eq. (2).

Figure 4 shows the double-logarithm curve, and the corresponding calculated results are given in Table 2. The apparent binding constants ($K_a$) between PAL–$Fe^{3+}$ and BSA were $5.633 \times 10^5\,\mathrm{M^{-1}}$ (290.15 K, $R = 0.9994$), $5.309 \times 10^5\,\mathrm{M^{-1}}$ (300.15 K, $R = 0.9995$), and $4.663 \times 10^5\,\mathrm{M^{-1}}$ (310.15 K, $R = 0.9998$), and the binding sites values ($n$) were $1.09 \pm 0.01$. The data clearly showed that the binding site on BSA for PAL–$Fe^{3+}$ was independent of temperature from 290.15 K to 310.15 K. The result illustrated that there was a strong binding force between PAL–$Fe^{3+}$ and BSA, and a binding site would be formed. The correlation coefficients are larger than 0.999, indicating that the interaction between PAL–$Fe^{3+}$ and BSA agrees well with the site-binding model underlying Eq. (2).

However, the binding constant between PAL–$Fe^{3+}$ and BSA with respect to the increasing temperature was noticed. From the temperature dependence of the binding equilibrium constants, it is possible to calculate values for the thermodynamic functions involved in the binding and dissociation process. The decrease in the binding constant with increase in temperature suggested the involvement of

**TABLE 1** **Fluorescence Quenching Constants of BSA by PAL in the Absence and Presence of $Fe^{3+}$**

| System | Temperature (K) | $K_{SV}$ ($\times 10^5\,\mathrm{M^{-1}}$) | $K_q$ ($\times 10^{13}$ $\mathrm{M^{-1}s^{-1}}$) | $R$ |
|---|---|---|---|---|
| BSA–PAL | 290.15 | 1.32 | 1.32 | 0.9967 |
| | 300.15 | 1.20 | 1.20 | 0.9990 |
| | 310.15 | 1.09 | 1.09 | 0.9974 |
| BSA–PAL–$Fe^{3+}$ | 290.15 | 1.82 | 1.82 | 0.9993 |
| | 300.15 | 1.64 | 1.64 | 0.9994 |
| | 310.15 | 1.44 | 1.44 | 0.9993 |

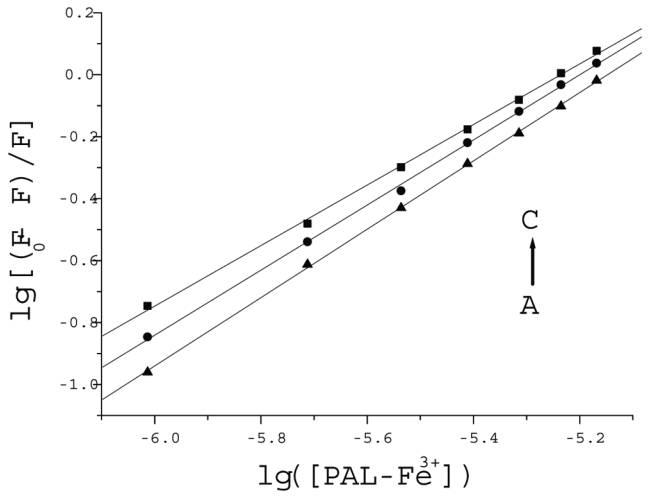


**FIGURE 4** **Double-log plot of fluorescence quenching of BSA by PAL–$Fe^{3+}$ at different temperature. From A to C: 290.15, 300.15, 310.15 K.**

**TABLE 2** The Binding Parameters for the System of PAL–$Fe^{3+}$ and BSA

| Temperature (K) | Binding constants ($\times 10^5\ M^{-}$) | Binding sites number ($n$) | $R$ |
|---|---|---|---|
| 290.15 | 5.633 | 1.09 | 0.9994 |
| 300.15 | 5.309 | 1.09 | 0.9995 |
| 310.15 | 4.663 | 1.09 | 0.9998 |

covalent interactions in the binding of PAL–$Fe^{3+}$ to BSA. The temperature may affect the stability of the PAL–$Fe^{3+}$–BSA system. The increasing temperature may result in the lower stability, which induced the above results. The decreased stability of the PAL–$Fe^{3+}$–BSA system played a fundamental role in the interaction with an increase in temperature.

## Thermodynamic Parameters and Nature of the Binding Forces

The interaction forces between biomacromolecules and medicines may involve hydrophobic forces, electrostatic interactions, van der Waals interactions, hydrogen bonds, and so forth. According to the data of enthalpy change ($\Delta H$) and entropy change ($\Delta S$), the model of interaction can be concluded[19]:

1. $\Delta H \approx 0$ and $\Delta S > 0$, hydrophobic forces;
2. $\Delta H < 0$ and $\Delta S < 0$, van der Waals interactions and hydrogen bonds;
3. $\Delta H < 0$ and $\Delta S > 0$, electrostatic interactions.

In order to elucidate the interaction of PAL–$Fe^{3+}$ with BSA, we calculated the thermodynamic parameters from Eqs. (3–5). If the temperature does not vary significantly, the enthalpy change ($\Delta H$) can be regarded as a constant. The free energy change ($\Delta G$) can be estimated from the following equation, based on the binding constants at different temperatures:

$$\Delta G = -RT \ln K_a \tag{3}$$

where $R$ is the gas constant, $T$ is the experimental temperature, and $K_a$ is the binding constant at the corresponding $T$. Then the enthalpy change ($\Delta H$) and entropy change ($\Delta S$) can be calculated from Eqs. (4) and (5):

$$\ln(K_2/K_1) = \Delta H(1/T_1 - 1/T_2)/R \tag{4}$$

**TABLE 3** The Thermodynamic Parameters of PAL–$Fe^{+}$–BSA Binding Procedure

| Temperature (K) | $\Delta H$ (kJ $mol^{-1}$) | $\Delta G$ (kJ $mol^{-1}$) | $\Delta S$ (J $mol^{-1}$ $K^{-1}$) |
|---|---|---|---|
| 290.15 | | −31.832 | 89.114 |
| 300.15 | −6.992 | −32.786 | 85.980 |
| 310.15 | | −33.549 | 85.668 |

where $K_1$ and $K_2$ are the binding constant at the experimental temperatures $T_1$ and $T_2$, respectively,

$$\Delta G = \Delta H - T\Delta S \tag{5}$$

The thermodynamic parameters for the interaction of PAL–$Fe^{3+}$ with BSA are shown in Table 3. Negative values of $\Delta G$ reveal that the binding process is spontaneous. Positive values of $\Delta S$ are evidence of hydrophobic interactions.[19] Moreover, a positive value of $\Delta S$ along with a negative $\Delta H$ value is characteristic of electrostatic interactions in aqueous solution. Thus, it is more likely that hydrophobic and electrostatic interactions are involved in the binding process. Consequently, hydrophobic interaction plays a major role in the binding of BSA and PAL in the presence of $Fe^{3+}$, but the electrostatic interaction cannot be excluded.

## Energy Transfer Between BSA and PAL in the Presence of Metal Ions

Lots of information concerning the molecular details of donor–acceptor pair can be obtained from nonradiative energy transfer.[16] The rate of energy transfer depends on the extent of the overlapping of the donor emission spectrum with the acceptor absorption spectrum, the relative orientation of the donor and acceptor transition dipoles, and the distance between these molecules. The dependence of energy transfer rate on interaction distance has been widely used to measure the distance between donors and acceptors. Generally, the maximum distance is in the range 7–10 nm.[16] According to the Föster nonradiation energy transfer theory,[16] the energy transfer effect is related not only to the distance between the acceptor and donor but also to the critical energy transfer distance ($R_0$):

$$E = R_0^6/(R_0^6 + r^6) \tag{6}$$

where $R_0$ is the critical transfer distance when the transfer efficiency is 50%, and $r$ is the mean distance between the centers of the donor and acceptor dipoles. Here the donor and acceptor are BSA and PAL–$Fe^{3+}$, respectively. $E$ is the energy transfer efficiency calculated from Eq. (7)

$$E = 1 - F/F_0 \tag{7}$$

where $F$ and $F_0$ are the fluorescence intensity of BSA with or without PAL–$Fe^{3+}$, respectively. $R_0$ can be given by

$$R_0^6 = 8.8 \times 10^{-25} K^2 \cdot N^{-4} \cdot \Phi \cdot J \tag{8}$$

Where $K^2$ is a factor describing the relative orientation in space of the transition dipoles of the donor and acceptor, $N$ is the refractive index of the medium, and $\Phi$ is the fluorescence quantum yield of the donor in the absence of acceptor. The overlap integral $J$ expresses the degree of spectral overlap between the donor emission and the acceptor absorption

$$J = \Sigma(F(\lambda) \cdot \varepsilon(\lambda) \cdot \lambda^4 \cdot \Delta\lambda)/\Sigma(F(\lambda) \cdot \Delta\lambda) \tag{9}$$

where $F(\lambda)$ is the fluorescence intensity of donor in wavelength $\lambda$ (dimensionless), and $\varepsilon(\lambda)$ is the molar absorption coefficient of the acceptor in wavelength $\lambda$ (with unit of $cm^{-1}\,mol^{-1}$). In this paper, $J$ can be evaluated by integrating the spectrum in Fig. 5 for $\lambda = 300$ to 500 nm.

Under these experimental conditions, the distance corresponding with 50% energy transfer from BSA to PAL–$Fe^{3+}$ can be estimated to $R_0 = 2.44$ nm from Eq. (8) using $K^2 = 2/3$, $N = 1.336$, and $\Phi = 0.15$.[16] Moreover, the energy transfer effect $E = 0.0594$ can be obtained from Eq. (7), and the binding distance between PAL–$Fe^{3+}$ and amino acid residue in BSA is $r = 3.90$ nm. Obviously, the distance is much lower than 7 nm, indicating that the static quenching interaction between PAL–$Fe^{3+}$ and BSA and the energy transfer from BSA to PAL–$Fe^{3+}$ occurs with high probability. For BSA, it has two tryptophan residues: hydrophobic amino acid residues, such as Trip-214, are located in the hydrophobic cavities of BSA and the additional tryptophan (Trp-135) is located on the surface of the molecule. In this paper, PAL–$Fe^{3+}$ is probably bound to Trp-214 residue mainly through the hydrophobic interaction according to the thermodynamic results. However, interaction between Trp-135 and PAL cannot be precluded.

Meanwhile, comparing the energy transfer efficiency ($E$) and distance between PAL–$Fe^{3+}$ and BSA, which is shown in Table 4 with our previous work,[11] it can be concluded that the influence of metal ions cannot be ignored. Molecular conformational transition of BSA caused by metal ions makes the original conformation more open,[20] so it is



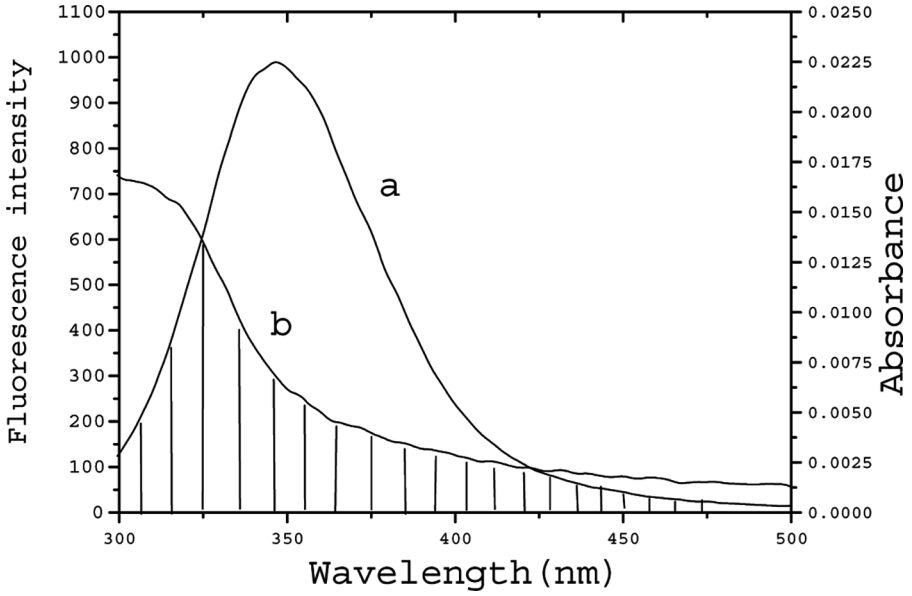


**FIGURE 5** Overlap spectra of PAL's UV absorption spectra (curve b) and BSA's fluorescence spectra (curve a). $C_{PAL} = 9.7 \times 10^{-7}$ mol/L; $C_{BSA} = 9.7 \times 10^{-7}$ mol/L.

**TABLE 4** *E* and *r* of PAL–BSA in the Absence and Presence of $Fe^{3+}$

| System | *E* | *r* |
|---|---|---|
| BSA–PAL | 0.0834 | 5.01 |
| BSA–PAL–$Fe^{3+}$ | 0.0594 | 3.87 |

easier for PAL–$Fe^{3+}$ segments to insert into the inner space of BSA. This would decrease the stereo-distance *r* between segments of PAL–$Fe^{3+}$ and fluorescent residues of BSA, then increase the energy transfer efficiency (*E*). The data of *r* and *E* as listed in Table 4 verifies this explanation. From *r* and *E* discussed above, it is possible that quenching efficacy of PAL is enhanced by metal ions because of the possible transition of BSA molecular conformation induced by metal ions.

## 2D CORRELATION ANALYSIS OF THE FLUORESCENCE ON THE INTERACTION BETWEEN BSA AND PAL IN THE PRESENCE OF Fe(III)

As can be seen from Fig. 2, BSA has strong fluorescence emission with a peak at 347 nm on excitation at 285 nm; upon the addition of PAL–$Fe^{3+}$, the fluorescence intensity was continuously decreased in protein. Using these spectra, we carried out the 2D analysis. The synchronous and asynchronous correlation maps are shown in Fig. 6.

The synchronous 2D spectrum of the sample shows a strong auto peak at 350 nm and a negative cross-peak at 347/460 nm; in the synchronous plot, diagonal peaks are referred to as auto peaks. The intensity of auto peaks is always positive, and they always represent the overall extent of the concentration-induced fluctuation of spectral intensity. Hence, the strong auto peak at 350 nm indicates the significant concentration-induced intensity variation of the spectral features at these positions vary greatly. This is due to the fact that both Trp bands reduce their intensities with increasing PAL–$Fe^{3+}$. It might be referred to a change in the conformation of tryptophan microregion caused by the interaction of BSA with PAL–$Fe^{3+}$. Through our previous work, Trp-214 residue plays an important structural role in the formation of the IIA binding site by limiting the solvent accessibility, and besides that it participates in

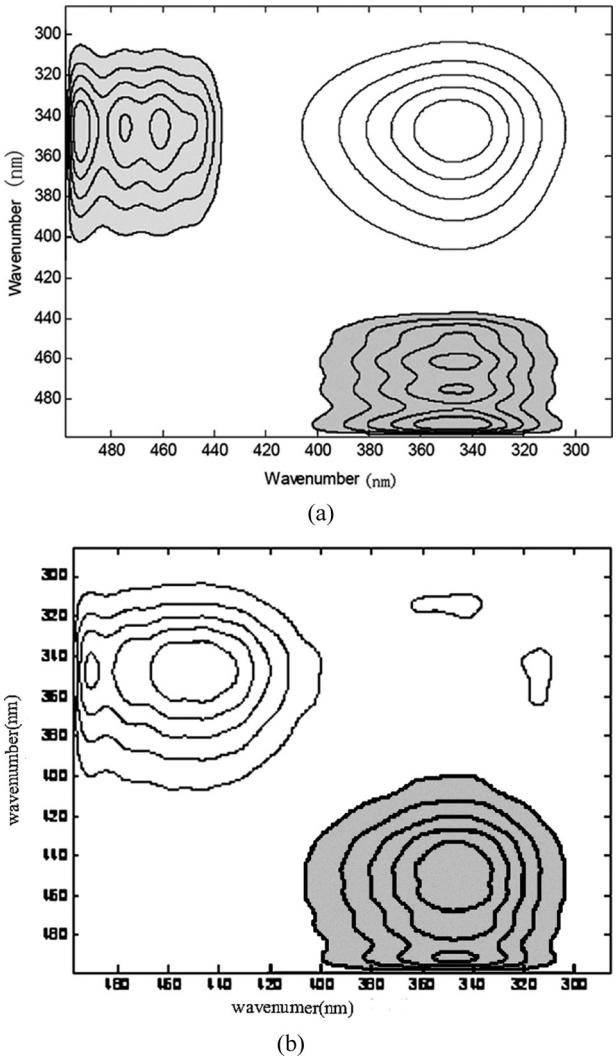


**FIGURE 6** Two-dimensional fluorescence correlation spectra of BSA and PAL–$Fe^{3+}$: (a) synchronous 2D fluorescence correlation map and (b) asynchronous 2D fluorescence correlation map.

additional hydrophobic packing interaction; after PAL–$Fe^{3+}$ segments insert into the hydrophobic region of BSA, PAL–$Fe^{3+}$, which structure changed, formed multimer and generated tenuous fluorescence.

An asynchronous plot has only off-diagonal peaks; the presence of asynchronous peaks indicates that the intensity responses of corresponding bands occur at different rates. A positive asynchronous peak at (v1, v2) means that the intensity at v1 changes faster compared with that at v2, whereas the negative asynchronous peak implies the opposite phenomenon. This feature is very useful in differentiating overlapped bands due to different spectral origin. There is a cross-peak at 347/460 in Fig. 6b; we realize that $\Phi$ (347, 460) $< 0$ and $\Psi$ (347,

$460) > 0$, where the symbols $\Phi$ and $\Psi$ denote synchronous and asynchronous peaks, respectively. According to Noda,[15] this fact indicates that the fluorescence of BSA changed its intensity before the structure change of PAL–$Fe^{3+}$.

## CONCLUSIONS

In this paper, the binding reaction between PAL and BSA has been investigated by using fluorescence spectroscopy, UV absorption spectra, and two-dimensional fluorescence correlation spectroscopy. The study of the interaction of PAL and BSA shows that a complex is formed between these species through the static quenching procedure. The binding constants and thermodynamic parameters were calculated according to the relevant fluorescence data. The binding study of drugs with proteins is of great importance in pharmacy, pharmacology, and biochemistry.

This study is expected to provide important insight into the interactions of the physiologically important protein BSA with drugs. Information is also obtained about the effect of environment on BSA structure, which may be correlated with its physiologic activity.



## REFERENCES


1. Elena, K. Interactions of human serum albumin with retinoic acid, retinal and retinyl acetate. *Biochem. Pharmacol.* **2007**, *73*, 901–910.
2. Lu, J. Q.; Jin, F.; Sun, T. Q.; Zhou, X. W. Multi-spectroscopic study on interaction of bovine serum albumin with lomefloxacin–copper(II) complex. *Int. J. Biol. Macromol.* **2007**, *40*, 299–304.
3. Neelam, S.; Sonu, B. Reversible binding of celecoxib and valdecoxib with human serum albumin using fluorescence spectroscopic technique. *Pharmacol. Res.* **2006**, *54*, 77–84.
4. Malonga, H.; Neault, J. F.; Riahi, H. A. Transfer RNA binding to human serum albumin: A model for protein–RNA interaction. *DNA Cell Biol.* **2006**, *25*, 393–398.
5. Mancuso, C.; Bonsignore, A.; Capone, C.; Di Stasio, E.; Pani, G. Albumin-bound bilirubin interacts with nitric oxide by a redox mechanism. *Antioxid. Redox Signal* **2006**, *8*, 487–494.
6. Carter, D. C.; Chang, B.; Ho, J. X.; Keeling, K.; Krishnasami, Z. Preliminary Crystallographic studies of four crystal forms of serum albumin. *Eur. J. Biochem.* **1994**, *226*, 1049–1052.
7. He, X. M.; Carter, D. C. Atomic structure and chemistry of human serum albumin. *Nature* **1992**, *358*, 209–215.
8. Jiang, C. Q.; Gao, M. X.; Meng, X. Z. Study of the interaction between daunorubicin and human serum albumin, and the determination of daunorubicin in blood serum samples. *Spectrochim. Acta A Mol. Biomol. Spectrosc.* **2003**, *59*, 1605–1610.
9. Lu, J. X.; Zhang, G. Z.; Wang, Y. M. The interaction of 5-fluorouracil with deoxyribonucleic acid and serum albumin. *Chin. J. Anal. Chem.* **2001**, *29*, 192–194.
10. Tang, S. H. Study of interaction between gelatin and copper (II) using synchronours fluorescence spectroscopy. *Photographic Sci. Photochem.* **2005**, *23*, 102–107.
11. Chen, C. Y.; Gu, X. T.; Zhou, J. H. Binding studies of paeonolum with bovine serum albumin using spectroscopic methods. *Spectroscopy* **2007**, *21*, 53–60.
12. Noda, I. Two-dimensional infrared spectroscopy of synthetic and biopolymers. *Bull. Am. Phys. Soc.* **1986**, *31*, 520.
13. Noda, I. Two-dimensional infrared spectroscopy. *J. Am. Chem. Soc.* **1989**, *111*, 8116.
14. Noda, I. Two-dimensional infrared (2-D IR) spectroscopy: Theory and applications. *Appl. Spectrosc.* **1990**, *44*, 550–561.
15. Noda, I. Generalized two-dimensional correlation method applicable to infrared, Raman and other types of spectroscopy. *Appl. Spectrosc.* **1993**, *47*, 1329–1336.
16. Sharma, A.; Schulman, S. G. *Introduction to Fluorescence Spectroscopy*; John Wiley & Sons: New York, 1999.
17. Lakowica, J. R.; Weber, G. Quenching of protein fluorescence by oxygen: Detection of structural fluctuations in macromolecules. *Biochemistry* **1973**, *12*, 4161–4170.
18. Huang, C. Z.; Li, K. A.; Tong, S. Y. Determination of nucleic acids by a resonance light-scattering technique with alpha, beta, gamma, delta-tetrakis [4-(trimethyl ammoniumyl) phenyl] porphine. *Anal. Chem.* **1996**, *68*, 2259–2263.
19. Ross, P. D.; Subramanian, S. Thermodynamics of protein association reactions: Forces contributing to stability. *Biochemistry* **1981**, *20*, 3096–3102.
20. Liang, H.; Ouyang, D.; Hu, X. Y.; Tai, J. Z.; He, J. T.; Zhou, Y. Q. Structural studies of on metal-serum albumin III. Slow conformational transition of HSA and BSA induced by $Ni^{2+}$ ion. *Acta Chim. Sinica* **1998**, *56*, 662–667.